Available online at www.sciencedirect.com

ScienceDirect

journal homepage: www.JournalofSurgicalResearch.com

Sinusoidal protection by sphingosine-1-phosphate receptor 1 agonist in liver ischemia-reperfusion injury

Takahiro Ito, MD,[a] *Naohisa Kuriyama, MD,*[a,*] *Hiroyuki Kato, MD,*[a] *Akitoshi Matsuda, MD,*[b] *Shugo Mizuno, MD,*[a] *Masanobu Usui, MD,*[a] *Hiroyuki Sakurai, MD,*[a] *and Shuji Isaji, MD*[a]

[a] *Department of Hepatobiliary Pancreatic and Transplant Surgery, Mie University Graduate School of Medicine, Tsu, Mie, Japan*

[b] *Department of Surgery, Mie Chuo Medical Center, Tsu, Mie, Japan*

ARTICLE INFO

Article history:
Received 1 July 2017
Received in revised form
20 September 2017
Accepted 29 September 2017
Available online xxx

Keywords:
Anti-inflammatory action
Sinusoidal blood flow
Vasorelaxation
Vascular integrity
Endothelial stabilization

ABSTRACT

Background: Functional and structural damages in sinusoidal endothelial cells (SECs) have a crucial role during hepatic ischemia-reperfusion injury (IRI). In regulating endothelial function, sphingosine-1-phosphate receptor 1 (S1PR1), which is a G protein–coupled receptor, has an important role. The present study aimed to clarify whether SEW2871, a selective S1PR1 agonist, can attenuate hepatic damage caused by hepatic IRI, focusing on SEC functions.

Methods: In vivo, using a 60-min partial-warm IRI model, mice were treated with SEW2871 or without it (with vehicle). *In vitro*, isolated SECs pretreated with SEW2871 or without it (with vehicle) were incubated with hydrogen peroxide.

Results: Compared with the IRI + vehicle group, SEW2871 administration significantly improved serum transaminase levels and liver damage, attenuated infiltration of Ly-6G and mouse macrophage antigen-1-positive cells, suppressed the expression of vascular cell adhesion molecule-1 and proinflammatory cytokines in the liver, and enhanced the expressions of endothelial nitric oxide synthase (eNOS) and vascular endothelial (VE) cadherin in the liver (eNOS/β-actin [median]: 0.24 *versus* 0.53, $P = 0.008$; VE-cadherin/β-actin [median]: 0.21 *versus* 0.94, $P = 0.008$). *In vitro*, compared with the vehicle group, pretreatment of SECs with SEW2871 significantly increased the expressions of eNOS and VE-cadherin (eNOS/β-actin [median]: 0.22 *versus* 0.29, $P = 0.008$; VE-cadherin/β-actin [median]: 0.38 *versus* 0.67, $P = 0.008$). As results of investigation of prosurvival signals, SEW2871 significantly increased Akt phosphorylation in SECs and decreased lactate dehydrogenase levels in supernatants of SECs.

Conclusions: These results indicate that S1PR1 agonist induces attenuation of hepatic IRI, which might be provided by preventing SEC damage. S1PR1 may be a therapeutic target for the prevention of early sinusoidal injury after hepatic IRI.

* *Corresponding author*. Department of Hepatobiliary Pancreatic and Transplant Surgery, Mie University Graduate School of Medicine, Edobashi 2-174, Tsu, Mie 514-8507 Japan. Tel.: +81 59-232 1111; fax: +81 59 232 8095.
E-mail address: naokun@clin.medic.mie-u.ac.jp (N. Kuriyama).

0022-4804/$ – see front matter
https://doi.org/10.1016/j.jss.2017.09.048

Introduction

Hepatic ischemia-reperfusion injury (IRI) is a serious cause of liver damage occurring during liver resection and transplantation and is the result of diverse and complex factors that involve the interaction among hepatocytes, sinusoidal endothelial cells (SECs), Kupffer cells, hepatic stellate cells, infiltrating neutrophils, macrophages and lymphocyte.[1,2] Among these cells in the liver, SECs are the first cells to direct the blood flow into the sinusoids and act as a primary barrier between the blood flow and parenchymal hepatocytes,[3] and thus they play the important protective roles controlling vascular homeostasis, inflammation, vascular tone, and toxicant clearance.

Sphingosine-1-phosphate receptor 1 (S1PR1), which is one of five receptors for sphingosine-1-phosphate (S1P) (lipid mediator), is expressed in a wide variety of tissues including endothelial cells and lymphocytes and has a role in regulating the endothelial barrier protection,[4] vascular tone,[5] cell survival signal activation,[6] and lymphocyte maturation/migration.[7] From a pharmacological point of view, S1PR1-selective agonists could serve as novel therapeutics. The development of the highly selective S1PR1 agonist, SEW2871, which was originally identified in 2004,[8] has enabled examination of S1PR1-mediated cell responses, using animal models such as renal IRI,[9,10] myocardial IRI,[11] heart transplant,[12] cardiopulmonary bypass,[13] and acute pancreatitis.[14] Using a renal IRI mouse model, Lien *et al.*[9] revealed that SEW2871 administration significantly attenuated renal damage by reducing neutrophil/macrophage infiltration and cytokine production in the kidney. In hepatic IRI models, however, there have been few studies on the effect of selective S1PR1 agonists.

To maintain normal sinusoidal circulation, vascular tone is important; endothelial nitric oxide synthase (eNOS) function in SECs plays an important physiological role in decreasing the portal pressure, attenuating storage/reperfusion injury, and improving microcirculation in sinusoids.[15] In addition, vascular integrity is also crucial. Vascular endothelial (VE) cadherin, which is a component of endothelial cell–cell adherence junctions, has a key role in the maintenance of vascular integrity. Recently, *in vitro* studies have revealed that S1PR1 has an important role in the upregulation of prosurvival signals in the endothelial cells.[16,17] To the best of our knowledge, there have been no previous studies on the effect of SEW2871 on liver damage induced by hepatic IRI using animal models, focusing on the role of SEC functions.

The aim of the present study was to clarify whether SEW2871 can attenuate hepatic damage produced by hepatic IRI in a mouse model, paying special attention to SEC functions such as the expression of eNOS, VE-cadherin, and prosurvival signals, using isolated SECs, in addition to the antiinflammatory effect.

Methods

Animals

Seven- to eight-week-old male C57BL/6 mice (21-26 g; Japan SLC Inc, Hamamatsu, Japan) were used. The experiments were reviewed and approved by the Animal Care and Use Committee at Mie University Graduate School of Medicine (No. 28-9) and conducted in compliance with the Guidelines for Animal Experiments in Mie University Graduate School of Medicine.

Partial hepatic IRI model

A warm hepatic IRI model was established in mice as reported previously.[18,19] Mice were anesthetized with isoflurane, and livers were exposed through a midline laparotomy. The arterial and portal venous blood supplies were interrupted to the cephalad lobes of the liver for 60 min using an atraumatic clip. The right hepatic lobe and the caudate lobe were perfused to prevent intestinal congestion. After 60 min of ischemia, the clip was removed, thus initiating hepatic reperfusion. Mice were sacrificed to collect blood and liver tissues at 4 h or 24 h after reperfusion.

Dose determination of SEW2871

SEW2871 (Cayman Chemical Company, Ann Arbor, MI) was dissolved in 100% dimethyl sulfoxide (DMSO) and diluted with 50% Tween 20 just before administration, and final concentration of DMSO was 20%, as described previously.[14] According to a pharmacokinetics study on SEW2871 administration by oral gavage in mice, lymphopenia, which is a major effect of SEW2871, was maintained for more than 12 h after oral administration.[8] To examine the effect of SEW2871 treatment on our hepatic IRI model using serum alanine transaminase (ALT) levels at 4 h after reperfusion, SEW2871 solution was administrated by oral gavage at several different doses and time points as shown in supplemental data 1. A dose of 25 mg/kg given at 12 h and 3 h before the ischemia induction had a significant effect: 1596 ± 281 IU/L in mice ($n = 4$) treated with SEW2871 *versus* 2317 ± 366 IU/L in mice ($n = 4$) treated with vehicle ($P = 0.029$). Because the effective duration of SEW2871 treatment measured by lymphopenia is about 12 h, we considered that additional administration at 12 h after reperfusion was required to maintain the treatment effects. Accordingly, we decided to give 25 mg/kg SEW2871 12 h and 3 h before ischemia induction and 12 h after reperfusion.

Experimental groups

Mice were randomly allocated to four groups

1) Sham + vehicle group: mice underwent laparotomy alone and were treated with vehicle alone (50% Tween with 20% DMSO)
2) Sham + SEW2871 group: mice underwent laparotomy alone and were treated with SEW2871 (25 mg/kg)
3) IRI + vehicle group: mice underwent 70% hepatic IRI and were treated with vehicle
4) IRI + SEW2871 group: mice underwent 70% hepatic IRI and were treated with SEW2871 (25 mg/kg)

All groups were given vehicle or SEW2871 by oral gavage three times, at 12 h and 3 h before ischemia induction and at 12 h after reperfusion.

Measurement of serum transaminases

Liver injury was evaluated by serum aspartate transaminase (AST) and ALT levels using a commercially available kit (Wako, Osaka, Japan), following the manufacturer's instructions.

Histology

Liver specimens were fixed with a 10% buffered formalin solution, embedded in paraffin and processed for hematoxylin and eosin (H&E) staining as previously reported.[19] Liver damage at 4 h was graded with Suzuki's score,[20] and the results were evaluated by averaging 10 scorings in 40 high-power fields per section. The degree of liver necrosis at 24 h was assessed in H&E-stained paraffin sections. H&E stains were digitally photographed, and the percentage of the necrotic area was quantified using NIH ImageJ software in a manner blind to the different experimental groups, as previously described.[21]

Immunohistochemistry

Liver specimens embedded in Tissue-Tek OCT compound (Miles, Elkhart, IN) and snap frozen in liquid nitrogen were used for immunostaining, as previously described.[19] Primary antibodies against mouse macrophage antigen-1 (MAC-1; BD Biosciences, San Jose, CA), Ly-6G (BD Biosciences), CD4 (BD Biosciences), vascular adhesion molecule-1 (VCAM-1; Santa Cruz Biotechnology Inc, Santa Cruz, CA) and VE-cadherin (Santa Cruz Biotechnology) were used at the optimal dilutions. The number of Ly-6G, MAC-1, and CD4-positive cells in 10 different randomized peripheral areas of the central vein was counted in 40 high-power fields per section, and the results were averaged.

Circulating lymphocyte counts

Blood cell counts were measured on a Sysmex XT-1800i Hematology Analyzer (Sysmex Corporation, Kobe, Japan). White blood cell differential counts were performed on peripheral blood smears stained with May-Giemsa stain. Two hundred cells were counted per smear, and absolute numbers of lymphocytes were calculated.

RNA extraction and real-time quantitative polymerase chain reaction (PCR)

We measured interferon *(IFN)*-γ, interleukin *(IL)*-6, tumor necrosis factor *(TNF)*-α, intercellular adhesion molecule 1 (*ICAM*-1), *VCAM-1* and β-*actin* mRNA levels using TaqMan Gene Expression Assays (Applied Biosystems, Foster City, CA), following the manufacturer's instructions. The cDNA prepared from total RNA extracted from the livers was subjected to real-time quantitative PCR on a 7300 Fast Real-Time PCR System (Applied Biosystems). The following probes were designed by Applied Biosystems: for *IFN*-γ, 5′-FAM d(GCCAAGTTTGAGGTCAACAACCCAC) NFQ-3′; for *IL*-6, 5′-FAM d(TGAGAAAAGAGTTGTGCAATGGCAA) NFQ-3′; for *TNF*-α, 5′-FAM d (CCACGTCGTAGCAAACCACCAAGTG) NFQ-3′; for *ICAM*-1, 5′-FAM d (ATCACCGTGTATTCGTTTCCGGAGA) NFQ-3′; for *VCAM*-1, 5′-FAM d (TCCACGTGGACATCTACTCTTTCCC) NFQ-3′; and for β-*actin*, 5′-FAM d (ACTGAGCTGCGTTTTACACCCTTTC) NFQ-3′. The mRNA expression levels of *IFN*-γ, *IL*-6, *TNF*-α, *ICAM*-1, and *VCAM-1* were normalized to that of β-*actin* mRNA.

Western blot analysis

Western blots were performed as reported previously.[22] Immobilon-P PVDF membranes (EMD Millipore, Bedford, MA) were incubated with specific antibodies against NOS3 (eNOS, Santa Cruz Biotechnology), VE-cadherin (Santa Cruz Biotechnology), phospho-Akt (Ser^{473}, p-Akt, Cell Signaling Technology, Beverly, MA), Akt (Cell Signaling Technology) and β-actin (Cell Signaling Technology). Prestained molecular weight markers (Protein MultiColor III; BioDynamics Laboratory, Tokyo, Japan) served as standards. Relative quantities of protein were determined using a densitometer (NIH ImageJ software).

Primary cell cultures of hepatocytes and sinusoidal endothelial cells

Primary SECs and hepatocytes were isolated from mice, as described previously.[18,23] To isolate primary murine SECs and hepatocytes, anesthetized mice were subjected to a midline laparotomy and cannulation of the inferior vena cava followed by liver perfusion with an ethylene glycol-bis(β-aminoethyl ether)-N,N,N′,N′-tetraacetic acid-chelating perfusion buffer (same composition as previously described[18]). After perfusion with 0.4% collagenase buffer, livers were minced and cells were dispersed in culture medium. Hepatocyte and nonparenchymal cells were separated using low-speed centrifugation methods. SECs were then purified using a two-step Percoll gradient (25/50%) and selective adherence.[24]

Isolated mouse hepatocytes (2×10^5 per well) were cultured in Roswell Park Memorial Institute medium with 10% fetal bovine serum in 24-well collagen-coated plates at 37°C with 5% CO_2 for 12 h. SECs (1×10^5 per well) were cultured in 24-well collagen-coated plates in endothelial growth medium at 37°C with 5% CO_2 for 24 h. Next, hepatocytes and SECs were separately incubated in Roswell Park Memorial Institute medium without fetal bovine serum and treated with vehicle (2% DMSO) or 20 μM SEW2871. The doses of SEW2871 were determined by evaluating Akt phosphorylation at 1 hour after treatment with SEW2871. (The results of examination for dose determination are shown in supplemental data 2.) After 1 h, 500-μM H_2O_2 was added to the medium, and then cells were incubated for 4 h. Before addition of medium and 4h after addition of H_2O_2, cell lysates were prepared for protein evaluation by zymography, and the supernatants were collected for cytotoxicity assay. Cell cytotoxicity was assessed by measuring the lactate dehydrogenase (LDH) levels in the supernatant. LDH were

assessed with the Cytotoxicity LDH Assay Kit-WST (Dojindo, Japan).

Immunofluorescence staining of sinusoidal endothelial cells

SECs were fixed in 4% paraformaldehyde and incubated with primary antibodies against VE-cadherin (Santa Cruz Biotechnology) or phospho-Akt (Cell Signaling Technology) at the optimal dilutions. Fluorescence signals were detected by Alexa Fluor 594 (Cell Signaling Technology) or Alexa Fluor 488 (Abcam, Cambridge, MA). Then, sections were mounted with ProLong Diamond Antifade Mountant with 4′,6-diamidino-2-phenylindole (Thermo Fisher Scientific Inc, San Jose, CA) for nuclear staining. Slides were observed through the appropriate filter using a BX51 fluorescence microscope (Olympus, Tokyo, Japan).

Data analysis

The results of continuous variables are expressed as medians and ranges. Differences between the distribution of the IRI + SEW2871 and IRI + vehicle groups were determined with the Mann–Whitney U test for unpaired comparison using SPSS (version 22). $P < 0.05$ was considered statistically significant.

Results

SEW2871 ameliorates hepatocellular injury

In the IRI groups, SEW2871 significantly reduced serum AST and ALT at 4h and 24h compared with vehicle group (AST at 4h: 3316 [2484-3909] IU/L in vehicle, 1688 [1022-2484] IU/L in SEW2871, $P = 0.016$, ALT at 4h: 3266 [2878-4000] IU/L in vehicle, 1353 [850-1677] IU/L in SEW2871, $P = 0.008$, AST at 24 h: 451 [148-661] IU/L in vehicle, 73 [45-167] IU/L in IRI + SEW2871, $P = 0.016$, and ALT at 24 h: 256 [141-320] IU/L in vehicle, 30 [15-102] IU/L in SEW2871, $P = 0.008$). In sham groups, there were no significant differences between vehicle and SEW2871 groups. (AST at 4h: 31 [14-33] IU/L in vehicle, 14 (9-17) IU/L in SEW2871, ALT at 4h: 3 [2-4] IU/L in vehicle, 3 [1-4] IU/L in SEW2871, AST at 24 h: 16 [10-36] IU/L in vehicle, 20 [14-23] IU/L in SEW2871, and ALT at 24 h: 3 [3-4] IU/L in vehicle, 3 [2-5] IU/L in SEW2871; Fig. 1).

As shown in Figure 2A, IRI livers mostly demonstrated sinusoidal vascular congestion at 4 h; however, livers treated with SEW2871 showed suppressed congestion at 4 h.

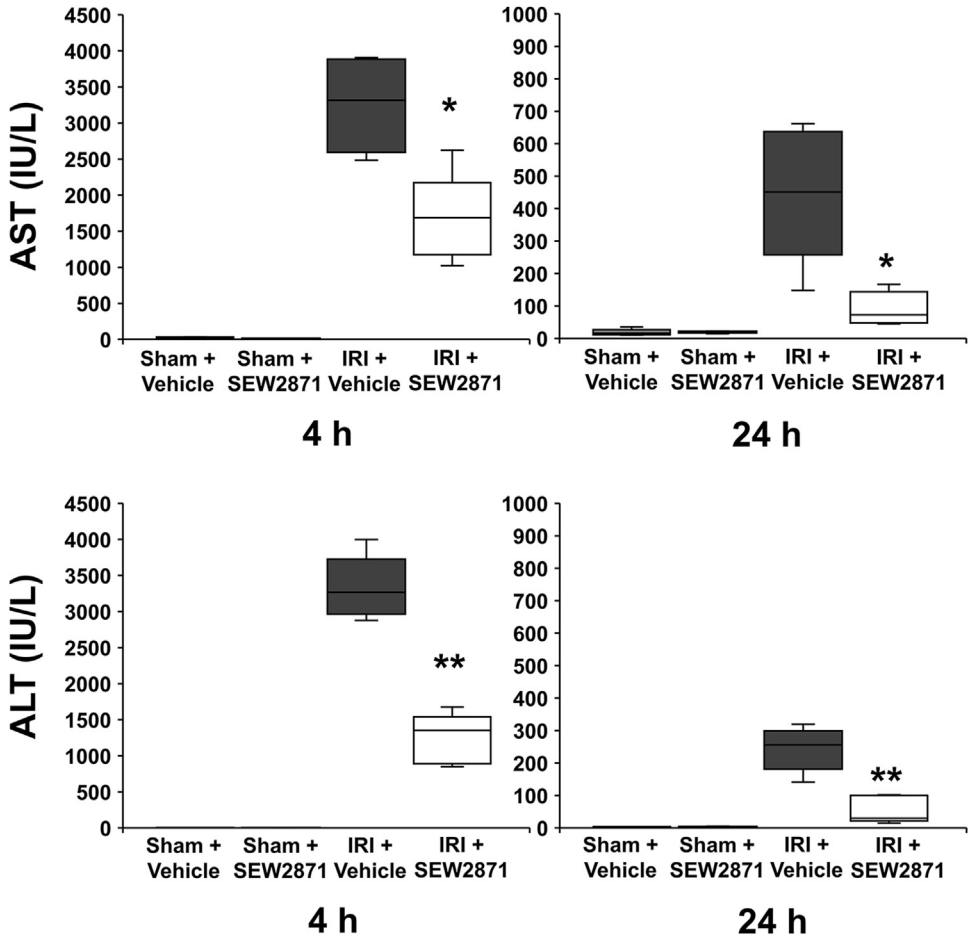

Fig. 1 – Liver transaminases in mice with or without SEW2871. Serum levels of AST and ALT in mice in IRI + SEW2871 group were significantly decreased compared with IRI + vehicle group at 4 h and 24 h after reperfusion. ($n = 5$ per group, $^{*}P < 0.05$ *versus* control, $^{**}P < 0.01$ *versus* IRI + vehicle group).

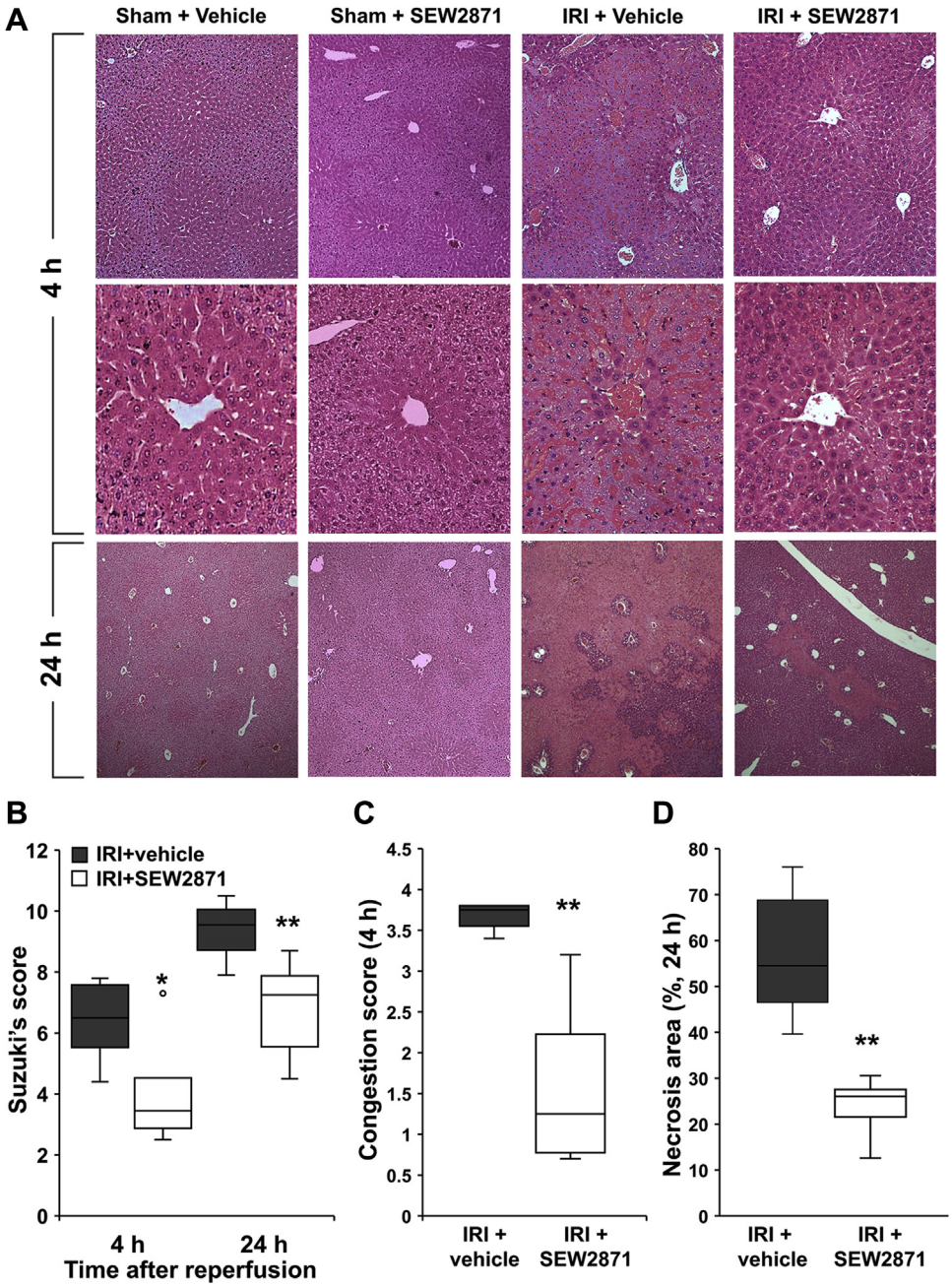

Fig. 2 – Hematoxylin and eosin staining of livers at 4 h and 24 h after IRI. IRI livers treated with only vehicle were mostly characterized by sinusoidal vascular congestion, whereas IRI livers with SEW2871 showed suppressed congestion at 4 h (panel A). Suzuki's scores in IRI + SEW2871 group at 4 h and 24 h were significantly lower than those in IRI + vehicle group (panel B). In particular, vascular congestion scores of Suzuki's criteria were markedly reduced in IRI livers with SEW2871 at 4 h (panel C). The percentage of hepatocellular necrosis in IRI livers (panel D) with SEW2871 at 24 h was significantly decreased compared with IRI livers with only vehicle (panel E). ($n = 6$ per group. $^{*}P < 0.05$ *versus* IRI + vehicle group, $^{**}P < 0.01$ *versus* IRI + vehicle group).

The Suzuki's scores of livers with IRI + SEW2871 at 4 h and 24 h were significantly lower than those of the IRI + vehicle group (4 h: 3.5 [2.5-7.3] *versus* 6.5 [4.4-7.8], $P = 0.026$; 24 h: 7.3 [4.5-8.7] *versus* 9.6 [7.9-10.5], $P = 0.004$; Fig. 2B). In particular, the vascular congestion scores of Suzuki's criteria were markedly lower for livers with IRI + SEW2871 at 4 h compared with the IRI + vehicle group (1.3 [0.7-3.2] *versus* 3.8 [3.4-3.8], $P = 0.002$; Fig. 2C). The percentage of hepatocellular necrosis in livers with IRI + SEW2871 at 24 h was significantly lower than that in IRI + vehicle group (26.0 [12.6-30.5] *versus* 54.5 [39.6-76.0], $P = 0.002$; Fig. 2D). We did not show Suzuki's score and necrosis area in sham group because the histological damage was not found in sham liver.

SEW2871 prevents intrahepatic inflammatory cell accumulation

We evaluated neutrophils and macrophage/monocyte infiltration by counting the number of Ly-6G, MAC-1, and CD4-positive cells in IRI livers, respectively. In sham liver with or without SEW2871, the number of Ly-6G, MAC-1, and CD4-positive cells were very small (Ly-6G at 4 h: 1.3 [0.6-1.9] in sham + vehicle, 1.3 [0.4-1.9] in sham + SEW2871, MAC-1 at 4 h: 2.3 [1.4-3.1] in sham + vehicle, 1.6 [0.9-3.1] in sham + SEW2871, CD4 at 4 h: 0.5 [0.3-0.6] in sham + vehicle, 0.3 [0.1-0.8] in sham + SEW2871, Ly-6G at 24 h: 2.7 [2.1-3.2] in sham + vehicle, 2.3 [0.8-3.4] in sham + SEW2871, MAC-1 at 24 h: 1.0 [0.3-1.7] in sham + vehicle, 1.4 [0.4-1.8] in sham + SEW2871, CD4 at 24 h: 0.7 [0.3-1.1] in sham + vehicle, 0.8 [0.2-1.6] in sham + SEW2871 per high-power field). In contrast, Ly-6G and MAC-1-positive cells markedly infiltrated into liver

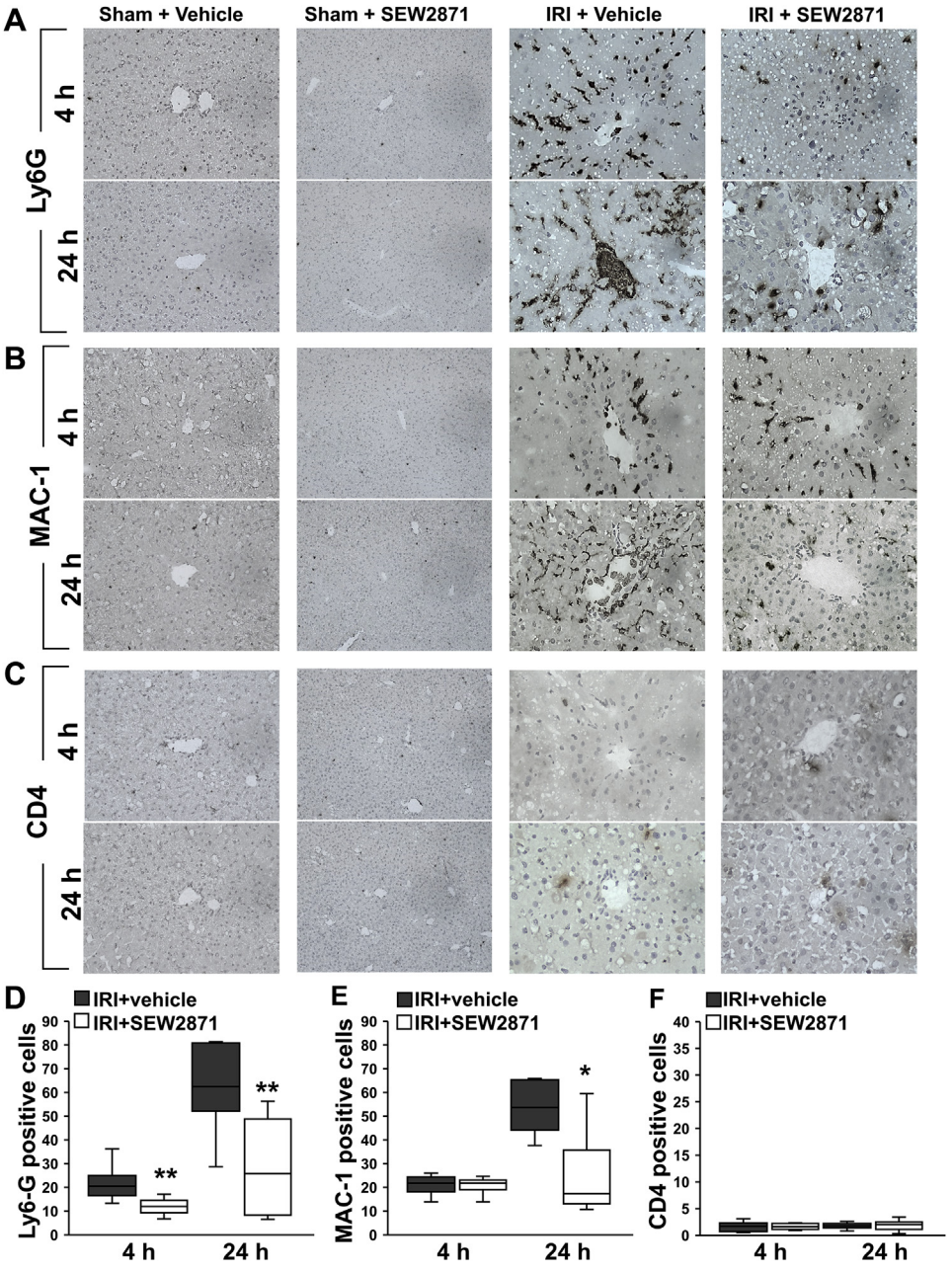

Fig. 3 – Inflammatory cells infiltration at 4 h and 24 h after reperfusion. The infiltration of Ly-6G-positive cells in the IRI liver with SEW2871 was significantly decreased as compared with IRI + vehicle group (panel A) at 4 h and 24 h (panel D). Although the number of MAC-1-positive cells in IRI liver at 4 h was not significantly different between IRI + vehicle and IRI + SEW2871 groups, at 24 h, their numbers in livers with SEW2871 were significantly lower than that in livers with control (panels B and E). The number of CD4-positive cells was not different between IRI + vehicle and IRI + SEW2871 groups (panels C and F). ($n = 6$ per group. $^{*}P < 0.05$ *versus* IRI + vehicle group, $^{**}P < 0.01$ *versus* IRI + vehicle group).

parenchyma. The number of Ly-6G-positive cells in SEW2871-treated IRI livers was significantly smaller than that in the livers of IRI + vehicle group at 4 h and 24 h (4 h: 12.0 [6.7-17.1] *versus* 20.6 [13.3-36.2], $P = 0.009$; 24 h: 25.8 [6.5-56.3] *versus* 62.4 [28.7-81.4], $P = 0.009$; Fig. 3A and D). There was no significant difference in the number of MAC-1-positive cells at 4 h between the IRI + vehicle and IRI + SEW2871 groups, whereas at 24 h the number was significantly smaller in the IRI + SEW2871 group than that in the IRI + vehicle group (4 h: 21.8 [13.9-24.7] *versus* 21.8 [13.9-26.0], $P = 0.937$, 24 h: 17.4 [10.7-59.5] *versus* 53.6 [37.6-65.9], $P = 0.026$; Fig. 3B and E). In contrast, the number of CD4-positive T cells in the IRI liver at 4 h and 24 h was very small in IRI + vehicle and IRI + SEW2871 groups, showing no significant difference (4 h: 1.6 [0.9-2.3] *versus* 1.7 [0.5-3.1], $P = 0.818$; 24 h: 2.0 [0.3-3.4] *versus* 1.8 [0.8-2.6], $P = 0.818$; Fig. 3C and F). When we counted the peripheral lymphocytes, the counts at 4 h in SEW2871-administered mice were significantly reduced compared with vehicle group in both of sham and IRI group (3465 [3027-4095]/μL in sham + vehicle, 464 [309-1529]/μL in SEW2871, 2067 [1954-2205] in IRI + vehicle, and 670 [595-935] in IRI + SEW2871 group, $P = 0.028$).

SEW2871 reduces the expression of proinflammatory cytokines

The mRNA expression of the cytokines, *IFN-γ*, *TNF-α*, and *IL-6*, was upregulated in IRI livers as compared with sham livers with or without SEW2871. In contrast, SEW2871 administration downregulated those expressions in IRI livers after 4 h of reperfusion compared with the IRI + vehicle group. In particular, the expression of *IFN-γ*, which is derived from T cells, was markedly suppressed by SEW2871 (*IFN-γ/β-actin* : 0.7 [0.2-1.2] in sham + vehicle, 0.7 [0.1-0.8] in sham + SEW2871, 5.0 [2.7-15.0] in IRI + vehicle, and 0.6 [0.3-1.0] in IRI + SEW2871, $P = 0.008$; *TNF-α/β-actin*: 0.5 [0.3-1.2] in sham + vehicle, 0.3 [0.1-0.9] in sham + SEW2871, 2.6 [2.2-2.9] in IRI + vehicle, and 1.7 [1.2-2.5] in IRI + SEW2871, $P = 0.032$; *IL-6/β-actin*: 0.2 [0.1-0.2] in sham + vehicle, 0.1 [0.01-0.7] in sham + SEW2871, 27.1 [11.6-51.9] in IRI + vehicle, and 6.7 [3.5-20.0] in IRI + SEW2871, $P = 0.016$; Fig. 4).

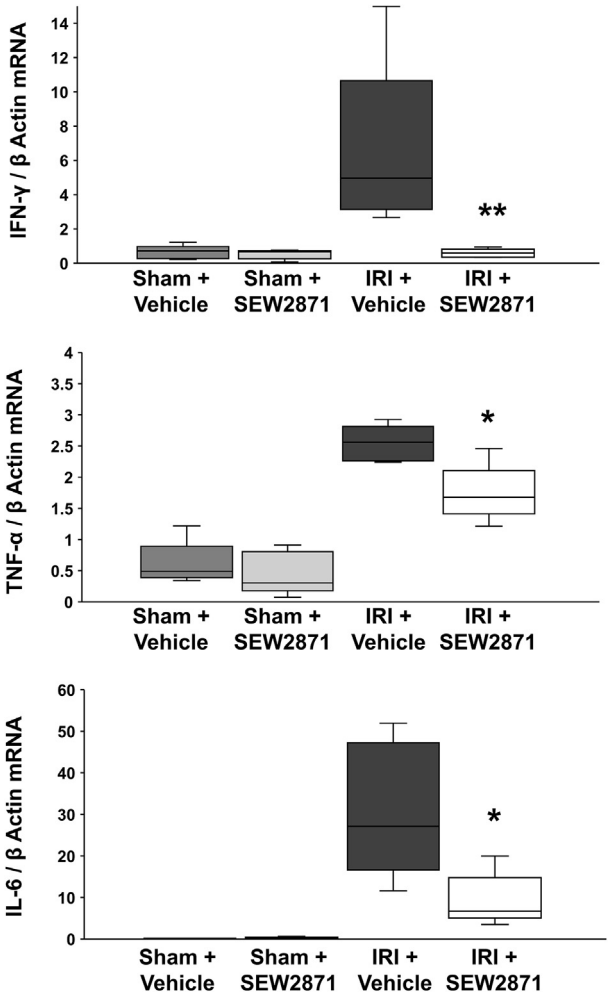

Fig. 4 – Proinflammatory cytokine expression in IRI livers with or without SEW2871. The mRNA expressions of cytokines (IFN-γ, TNF-α, and IL-6) were downregulated in IRI livers with SEW2871 at 4 h after reperfusion compared with those of IRI + vehicle group, respectively. In particular, IFN-γ which possibly derived from T cells was markedly reduced by SEW2871. ($n = 4$-5 per group. $^{*}P < 0.05$ *versus* IRI + vehicle group, $^{**}P < 0.01$ *versus* IRI + vehicle group).

SEW2871 suppresses the expression of vascular adhesion molecules

The mRNA levels of *VCAM-1* were significantly increased in IRI liver compared with those in the sham liver, and they were reduced in SEW2871-treated IRI livers at 4 h compared with those in IRI + vehicle group (*VCAM-1/β-actin*: 0.4 [0.2-0.8] in sham + vehicle, 0.3 [0.05-0.5]in sham + SEW2871, 5.4 [4.4-5.9] in IRI + vehicle, and 3.7 [3.1-4.4] in IRI + SEW2871, $P = 0.016$; Fig. 5A). Furthermore, immunohistochemistry showed that *VCAM-1* protein expression was low in sham livers with or without SEW2871, whereas it was expressed along the endothelium in IRI livers. SEW2871 treatment reduced its expression (Fig. 5B). In contrast, the mRNA levels of *ICAM-1* did not show any differences between the two groups (data not shown).

SEW2871 improves the expression of eNOS and VE-cadherin

In IRI livers, the eNOS expression was remarkably suppressed compared with the sham livers. However, SEW2871 administration significantly increased the expression of eNOS in the IRI livers at 4 h compared with the IRI + vehicle group (eNOS/*β-Actin*: 1.04 [1.03-10.6] in sham + vehicle, 1.04 [1.02-1.07] in sham + SEW2871, 0.24 [0.20-0.38] in IRI + vehicle, and 0.53 [0.40-0.74] in IRI + SEW2871, $P = 0.008$; Fig. 6A and C). In addition, when we examined the expression of VE-cadherin by immunostaining, it was strongly expressed along the sinusoidal area in the sham liver, whereas its expression was very low in IRI livers at 4 h. SEW2871 treatment, however, improved the expression of VE-cadherin (Fig. 6B). Consistently, Western blot analysis demonstrated that the

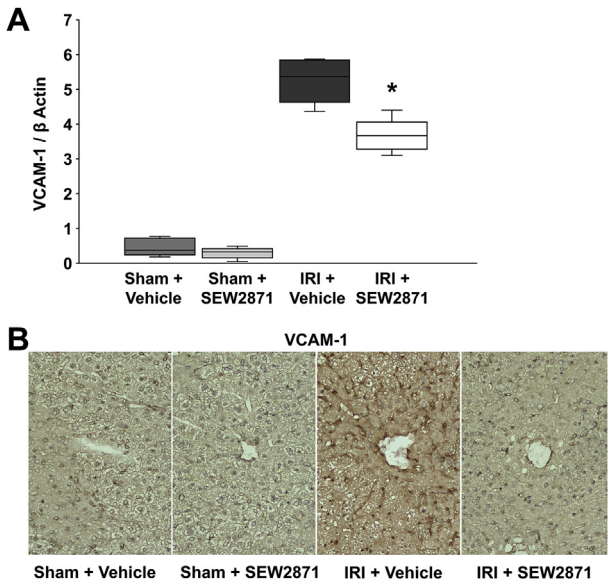

Fig. 5 – Adhesion molecule expression in IRI livers with or without SEW2871. The mRNA levels of VCAM-1, adhesion factors of inflammatory cells, were significantly reduced in IRI livers with SEW2871 at 4 h (panel A). In immunohistochmical section, there was almost no VCAM-1 expression in sham livers with or without SEW2871 (panel B), it was expressed along the endothelium in IRI livers. SEW2871 reduced its expression as compared with IRI + vehicle group. ($n = 5$ per each groups. $^*P < 0.05$ *versus* IRI + vehicle group).

expression of VE-cadherin was remarkably decreased in IRI livers with vehicle compared with sham liver (Fig. 6D), and it was significantly higher in SEW2871-administered IRI livers than in the IRI + vehicle group (VE-cadherin/*β-Actin*: 1.01 [0.95-1.07] in sham + vehicle, 1.04 [1.01-1.07] in sham + SEW2871, 0.21 [0.18-0.44] in IRI + vehicle, and 0.94 [0.53-1.19] in IRI + SEW2871, $P = 0.008$).

SEW2871 ameliorates the expression of the eNOS and VE-cadherin in sinusoidal endothelial cells treated with H_2O_2 in vitro

We investigated whether the effect of SEW2871 *in vivo* was directly provided to SECs. The primary cultured mouse SECs formed a triangle- or cone-shaped configuration in close contact with each other, as seen in the phase contrast microscope image. The cells and cell attachments were broken after the addition of 500-μM H_2O_2. Treatment with 20-μM SEW2871 decreased the destruction of cell morphology and arrangement (Fig. 7A). The immunofluorescent staining revealed a strong expression of VE-cadherin in the cells that were not exposed to H_2O_2. Treatment of H_2O_2 significantly decreased this expression; however, SEW2871 maintained continuous expression (Fig. 7B). When we quantified the expression of eNOS and VE-cadherin using Western blotting analysis, we found that these proteins were strongly expressed, regardless of addition of SEW2871 (eNOS/*β-actin*: 0.91 [0.83-1.05] in vehicle and 0.93 [0.84-1.23] in SEW2871, $P = 0.690$; VE-cadherin/*β-actin*: 1.31 [1.16-1.46] in vehicle and 1.39 [1.10-1.44] in SEW2871, $P = 0.548$). Addition of 500-μM H_2O_2 strongly decreased the expression of these proteins after 4 h; however, treatment with 20-μM SEW2871 significantly ameliorated the expression of eNOS and VE-cadherin compared with control (eNOS/*β-actin*: 0.22 [0.20-0.23] in vehicle, 0.29 [0.24-0.36] in SEW2871, $P = 0.008$; VE-cadherin/*β-actin*: 0.38 [0.34-0.51] in vehicle, and 0.67 [0.52-0.69] in SEW2871, $P = 0.008$; Fig. 7C-E).

SEW2871 activates Akt and inhibits cell toxicity of sinusoidal endothelial cells in vitro

The expression of p-Akt after 1 h in the presence of 20-μM SEW2871 was significantly higher when compared with that in the absence of SEW2871 (p-Akt/total Akt (t-Akt): 0.49 [0.45-0.63] in vehicle and 0.86 [0.81-1.29] in SEW2871, $P = 0.008$; Fig. 8A and C). The SEW2871-induced p-Akt expression was in the cytoplasm as demonstrated by immunofluorescent staining (Fig. 8B). Although t-Akt and p-Akt expression decreased after treatment with H_2O_2, the level of induction of Akt phosphorylation by SEW2871 was maintained at 4 h after the addition of H_2O_2 (p-Akt/t-Akt: 0.38 [0.27-0.54] in vehicle and 0.87 [0.62-1.00] in SEW2871, $P = 0.008$). Finally, the LDH levels in the supernatant of SEW2871-treated cultures 4 h after H_2O_2 addition were significantly lower compared with those in the vehicle group (the rate of LDH levels to vehicle group: 100 [92.9-111.6] % in vehicle and 72.4 [60.8-93.8] % in SEW2871, $P = 0.016$; Fig. 8D). We performed the same experiments on hepatocyte cultures; however, SEW2871 administration did not exert any effects (data not shown).

Discussion

In the present study using partial warm IRI model, a selective S1PR1 agonist SEW2871 significantly improved serum transaminase levels and liver histological damage, attenuated infiltration of Ly-6G and MAC-1-positive cells, suppressed the expression of VCAM-1 and proinflammatory cytokines in the liver, and improved eNOS and VE-cadherin in the liver. Moreover, *in vitro* study using isolated mice SEC, SEW2871 remarkably suppressed the decrease in eNOS and VE-cadherin expression induced H202 and increased Akt phosphorylation.

Effects of SEW2871 can be classified into three major pathways through regulation of inflammatory/immune cells migration, endothelial protection, and induction of cell pro-survival signals. In hepatic IRI models, there have been few studies on the effects of selective S1PR1 agonists. In 2010, using a mouse hepatic IRI model, Park *et al.*[25,26] demonstrated that S1P, which is one of sphingolipid metabolites, reduced liver and kidney injury after hepatic IRI by attenuating neutrophil infiltration, reducing plasma IL-6 and TNF-α upregulation, and preserving liver and kidney vascular integrity by reducing liver and kidney F-actin degradation. Furthermore, they revealed that the protective effect of S1P on liver and kidney injury after hepatic IRI was blocked by an S1PR1 antagonist, whereas a selective S1PR2 or S1PR3 antagonist had no effect. It is considered that selective S1PR1 activation plays

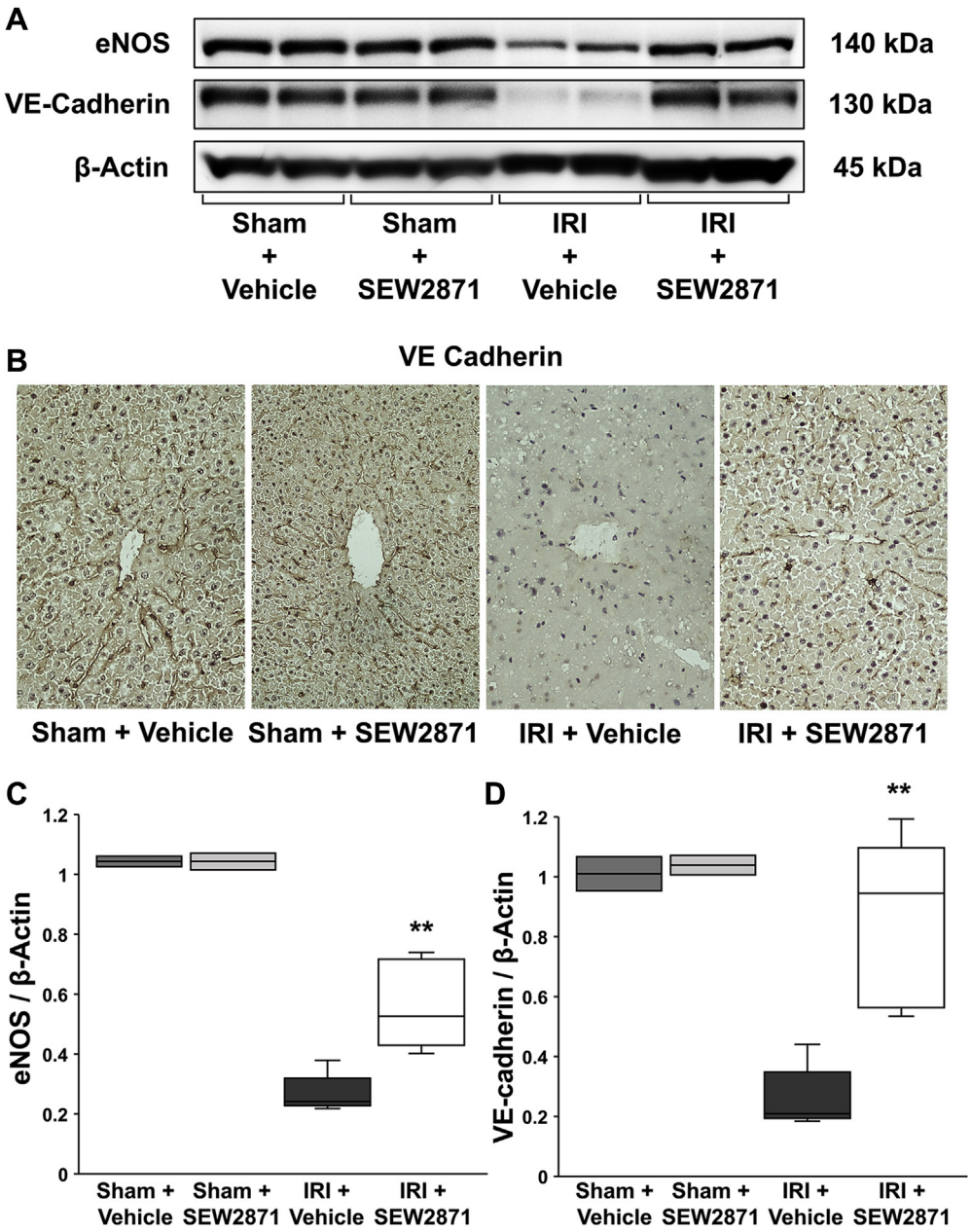

Fig. 6 – SECs damage and its protection by SEW2871 in IRI livers. SEW2871 increased the expression of eNOS in IRI livers at 4 h as compared with IRI + vehicle group (panels A and C). In addition, VE-cadherin in sham livers of mice by using immunostaining was highly expressed along the sinusoidal area (panel B). The expression of VE-cadherin was decreased in IRI livers with vehicle. SEW2871 prevented the reduction of VE-cadherin expression. As a result of Western blot analysis, VE-cadherin expressions in IRI + vehicle group were significantly higher than those in IRI + vehicle group (panels A and D). ($n = 2$ [sham] $n = 5$ [IRI group]. $^{**}P < 0.01$ *versus* IRI + vehicle group).

a pivotal cytoprotective role in hepatic IRI models. However, detailed mechanism of the effect of SEW2871 in the liver, especially in the SECs, has remained unclear.

When we confirm the antiinflammatory effect, SEW2871 administration significantly decreased the infiltration of neutrophils/macrophages into the liver. Concurrently, it reduced the expression of proinflammatory cytokines and adhesion molecules, which is consistent with a previous report.[25] There have been very few reports on hepatic IRI using SEW2871, although there have been several reports on renal IRI models. Lien *et al.*[9] have revealed that SEW2871 administration to renal IRI models significantly reduced neutrophil/macrophage infiltration and cytokine production in the kidney. They suggested that the renoprotective effect of SEW2871 was associated with the reduction in circulating lymphocytes and the suppression of the proinflammatory genes, *TNF-α*, *ICAM-1*, and *P-selectin* in renal tissue. It is well known that SEW2871 administration causes lymphopenia by retaining lymphocytes in secondary lymphoid organs such as lymph nodes and spleen, and it suppresses T cell infiltration into the target

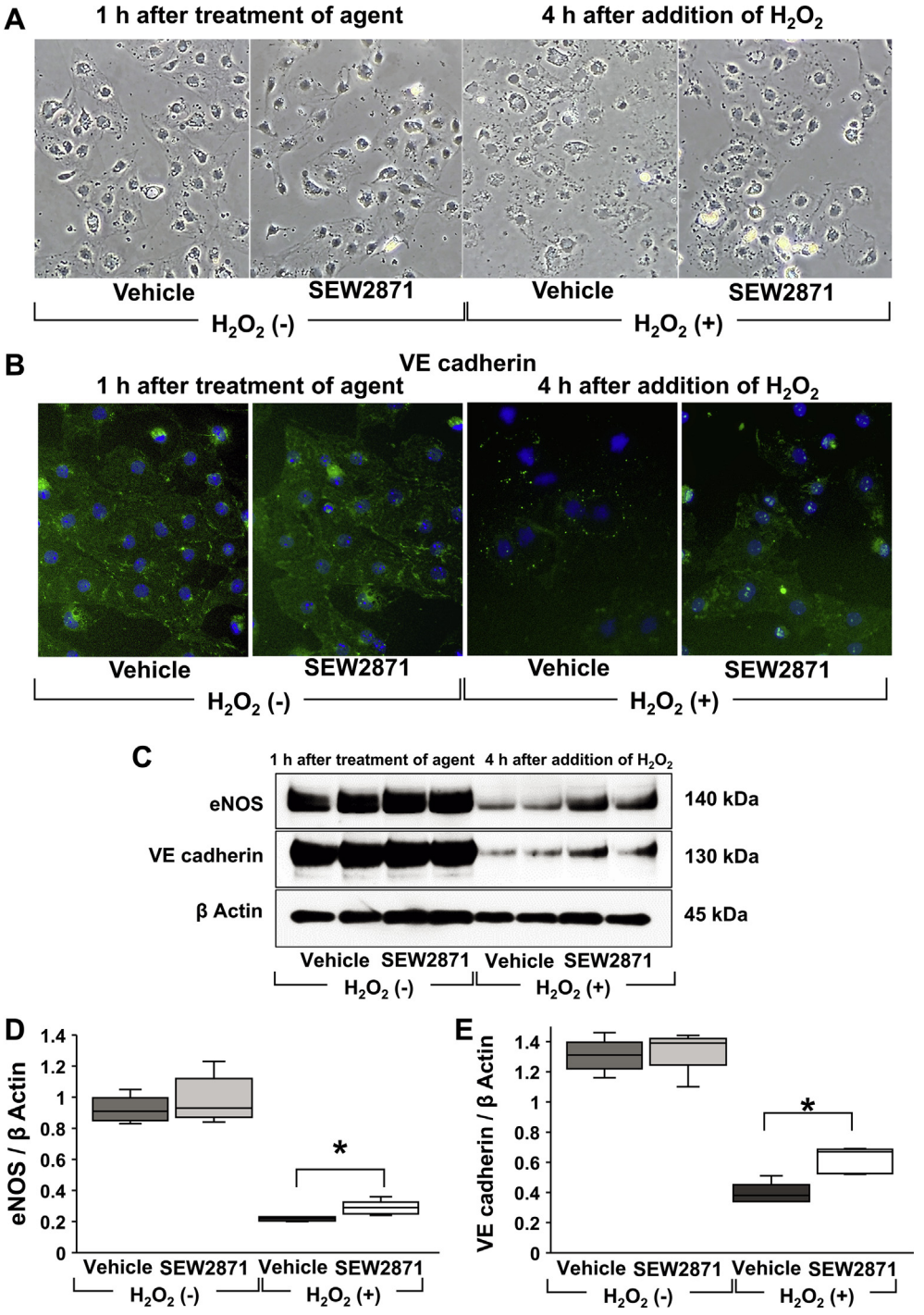

Fig. 7 – Direct effect of SEW2871 on SECs *in vitro*. In phase contrast microscope image, primary cultured mice SECs formed a triangle- or cone-shaped configuration in close contact with each other (panel A [left]). After addition of 500-μM H_2O_2, the cells and cell attachments were broken; however, the treatment of 20-μM SEW2871 decreased the destruction of cell form and arrangement (panel A [right]). In immunofluorescence staining, the expressions of VE-cadherin were strongly detected along cell under condition without H_2O_2. H_2O_2 extremely decreased its expressions, and SEW2871 maintained its continuous expression (panel B, VE-cadherin [green]). In Western blotting analysis, eNOS and VE-cadherin were strongly expressed, and the addition of SEW2871 was not affected under condition without H_2O_2 (panel C-E [left]). Although addition of 500-μM H_2O_2 decreased the expression of eNOS and VE-cadherin at 4 h after, treatment of 20-μM SEW2871 significantly suppressed the reduction of those expressions (panel C-E [right]). ($n = 5$ per group. $^*P < 0.01$).

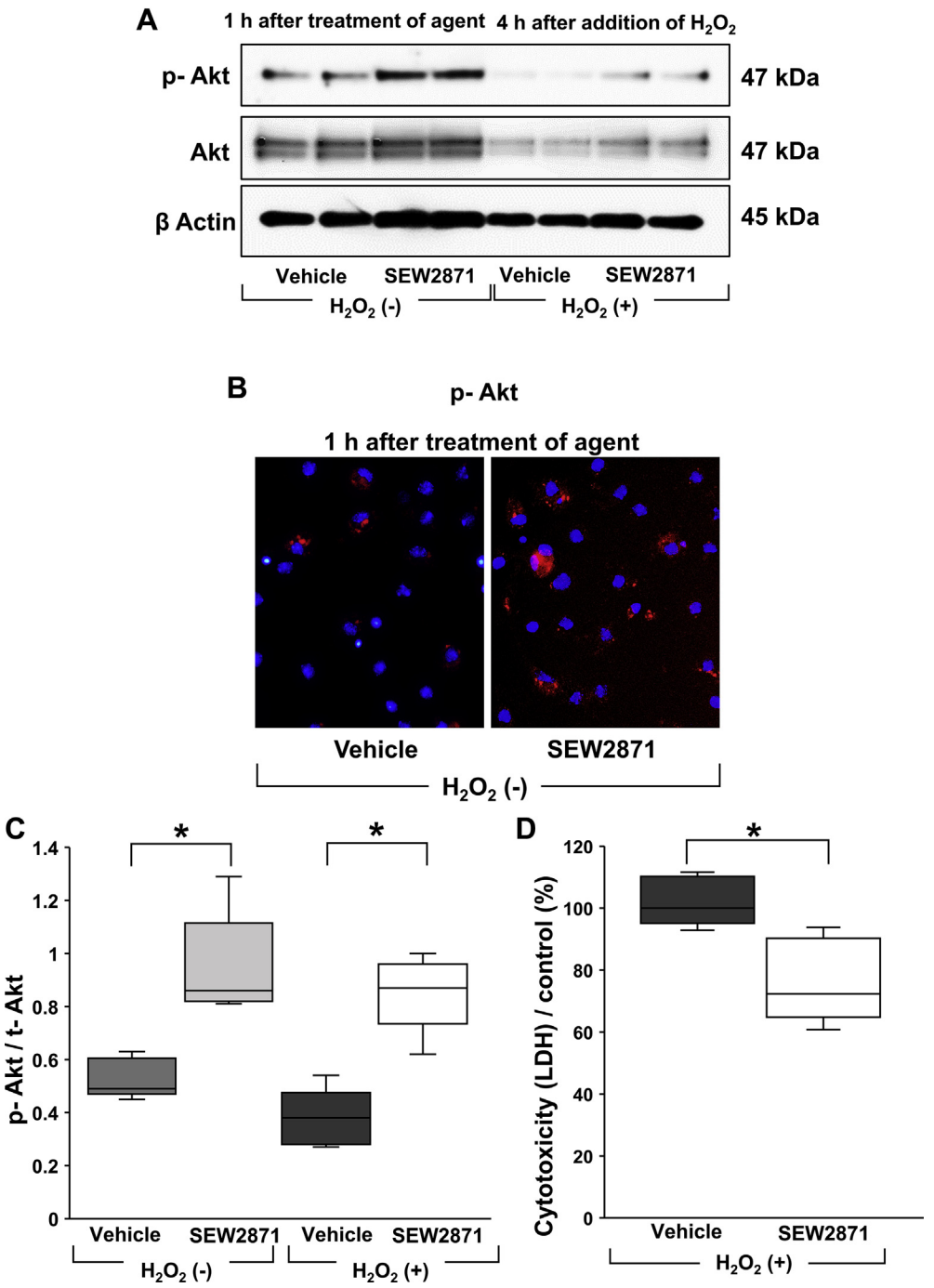

Fig. 8 – Survival signal by SEW2871 on SECs *in vitro*. The expression of p-Akt in the presence of 20-μM SEW2871 at 1 h after addition of the agent was significantly higher than that in the absence of SEW2871 (only vehicle) (panels A and C [left]). The acceleration of p-Akt expressions by SEW2871 was confirmed in cytoplasm by immunofluorescence staining (panel B, p-Akt [red]). Although t-Akt and p-Akt signaling were decreased by the addition of 500-μM H_2O_2, the acceleration of Akt phosphorylation by SEW2871 was maintained at 4 h after the addition of H_2O_2 (panels A and C [right]). Moreover, LDH levels in supernatant treated with SEW2871 at 4 h addition of H_2O_2 were significantly lower than those supernatant treated without SEW2871. (panel D). ($n = 5$ per group. $^*P < 0.01$).

organs. In the present study, peripheral lymphocyte counts at 4 h after reperfusion of SEW2871-treated mice were significantly decreased compared with the control, whereas the number of CD4-positive T cells in the liver at 4 h and 24 h was very low in both groups, showing no significant differences. Using a mouse renal IRI model to examine the effects of SEW2871, Lien *et al.*[9] have reported that the number of T cells in the kidney at 24 h after IRI was very low, and they could not detect any significant suppression of T cell infiltration. However, in a subsequent report from the same institution using

the same model,[10] they examined T cell infiltration into kidneys treated with SEW2871 at earlier time points, revealing that T cell infiltration was significantly reduced at 1 h and 4 h after reperfusion compared with the control. Using a mouse hepatic IRI model, Martin *et al.*[27] have reported that the administration of FTY720, which activates four S1P receptors, S1PR1, S1PR3, S1PR4, and S1PR5, prevented T cell infiltration into the liver 20 min after reperfusion. In the present study, we detected very few CD4-positive T cells in the liver both at 4 h and 24 h after IRI. If we evaluated T cell infiltration into the liver at earlier time points, the number of T cells in the liver may have been significantly different. In our model, we speculated that a decrease in circulating lymphocytes by SEW2871 contributed to a marked decrease in *IFN-γ* expression in the liver. Hence, one of the cytoprotective effects of SEW2871 was associated with reduction in circulating lymphocytes as in the previous reports.[9,10]

Several studies have reported that the role of S1P/S1PR1 maintained vascular tone by eNOS activation. Samarska *et al.*[13] have reported that the activation of S1PR1 promotes vasorelaxation responses in vessels, such as coronary artery and mesenteric artery, because of vascular NO synthesis derived from eNOS activation. Zheng *et al.*[28] have reported that S1P, which is one of the bioactive lipids of S1PR1, protected SECs from ethanol-induced injury in primary cultures and isolated perfused rat livers, and that the protective effect of S1P was mediated by the activation of eNOS. In the liver, stimulation of eNOS function in SECs plays an important physiological role in decreasing the portal pressure, attenuating storage/reperfusion injury and improving microcirculation in sinusoids.[15]

In addition, vascular integrity is important to maintain normal blood circulation and suppress inflammatory cell infiltrations to liver parenchyma. VE-cadherin has a key role in the maintenance of vascular integrity. Because of the association between S1PR1 and VE-cadherin, it has been considered that S1P affects endothelial cell–cell junctions by regulating assembly and expression of VE-cadherin.[29] Tobia *et al.*[30] have examined the role of S1PR1 in vascular development using zebrafish; S1PR1 downregulation by antisense morpholino oligonucleotide injection caused downregulation of VE-cadherin, resulting in lack of blood circulation. They concluded that the S1PR1/VE-cadherin pathway controls venous vascular integrity.

Taken together, it appears that S1PR1 activation by SEW2871 promotes eNOS and VE-cadherin maintenance, resulting in vasorelaxation and maintenance of vascular integrity. In the present study, therefore, we examined whether or not SEW2871 enhanced the expression of eNOS and VE-cadherin using a hepatic IRI model. In IRI livers, eNOS expressions were remarkably decreased compared with the sham livers. SEW2871 significantly increased the eNOS expressions compared with the control. Immunohistochemical examination revealed that VE-cadherin was highly expressed along the sinusoidal area in the sham livers, whereas its expression was low in IRI (control) livers. SEW2871 administration significantly increased the expression of VE-cadherin compared with the control. Moreover, sinusoidal congestion in IRI liver was remarkably improved by SEW2871; hence, it was considered that SEW2871 contributes to the maintenance and improvement of sinusoidal endothelium functions, although it was necessary to verify whether this effect which provided normal function to SECs by SEW2871 *in vivo* was a direct effect or as a result of antiinflammatory actions. Accordingly, we investigated the direct effect of SEW2871 on SECs *in vitro* to confirm the effect of *in vivo* study.

Using isolated mouse SEC cultures exposed to H_2O_2, we examined whether SEW2871 maintained eNOS and VE-cadherin expression in SECs in an environment not affected by inflammation actions such as lymphocytes and cytokines. In this study, primary cultures of mouse SECs exposed to H_2O_2 for 4 h showed broken cells and cell attachments; however, SEW2871 treatment decreased the destruction of cell morphology and arrangement. Moreover, SEW2871 treatment suppressed the H_2O_2-induced decrease in eNOS and VE-cadherin expression in SECs. These results support our *in vivo* results and the hypothesis that SEW2871 directly affects the maintenance of eNOS and VE-cadherin expression in SECs.

Among the previously mentioned three major pathways affected by the S1PR1-selective agonist, we examined the prosurvival signals in SECs. Herein, the expression of p-Akt was significantly enhanced 1 h after SEW2871 addition, and the levels of LDH in the supernatant were significantly lower than those in the control at 4 h after H_2O_2 addition. These results suggest that SEW2871 stimulated prosurvival signals in SECs. There have been no previous reports on the direct effects of SEW2871 using isolated SECs as a model organism. In agreement with our study, Nowatari *et al.*,[16] using a human SEC-cultured model, have demonstrated that S1P induced SEC proliferation through activation of Akt and suppressed SEC apoptosis, although which S1P receptor of the five receptors was involved was not elucidated. Argraves *et al.*,[17] using cultured human umbilical vein endothelial cells, have reported that high-density lipoprotein, which is a major plasma carrier of S1P, stimulated Akt activation and that this effect was blocked by an S1PR1 antagonist.

As for intercellular downstream signaling of S1PR1, several previous studies report that S1PR1 is coupled to Gi and ribosylate adenylyl cyclase and activates several intercellular signaling such as Ras/mitogen-activated protein kinase,[31] phosphoinositide 3-kinase (PI3K)/Akt, and eNOS pathway.[32] In addition, PI3K/Akt pathways and the eNOS pathway are considered to be involved in the regulation of apoptosis in endothelial cells including SECs.[16,28,32] Nowatari *et al.*[16] demonstrated that the inhibition of PI3K by LY294002 abolished the antiapoptotic effect of S1P on SEC by decreasing the Bcl-2 expression and increasing the Bax expression, whereas the inhibition of mitogen-activated protein kinase by PD98059 or eNOS by L-NAME did not. They suggested that PI3K/Akt pathway plays a central role in the antiapoptotic effect of S1P. Therefore, we hypothesized that S1PR1 agonism also plays an important role in the upregulation of prosurvival signals in hepatic IRI. However, *in vivo*, the expression of p-Akt in IRI liver exposed to SEW2871 was not significantly different from that in IRI + vehicle group (data not shown). At this point, we speculate that the p-Akt expression in the liver may be strongly influenced by hepatocytes that were not affected by SEW2871 under our experimental conditions and account for about 80% of the liver.

There are two limitations in our present study. First, SEC-specific S1PR1 transgenic mice are necessary for confirming whether SEW2871 has direct effects on SECs *in vivo*; however, SEC-specific S1PR1 transgenic mice are currently not available. Moreover, our present study could not use deficient or knockout mice. If endothelial-specific inducible knockout mice,[33] VE-cadherin, eNOS, or T cell-deficient/knockout mice can be used, more detail and precise mechanisms of the effect of SEW2871 *in vivo* will be clarified. Instead of knockout mice, we used primary cultured SECs to study the direct effect of SEW2871. Second, we could not confirm the effects of the inhibitors of S1PR1. A previous report[34] by using mice renal IRI models demonstrated that mice treated with a specific S1PR1 antagonist (W146) showed exacerbated renal and hepatic injury after renal IRI. In addition, another previous report[35] revealed that NIBR-0213, another selective S1PR1 antagonist, induced dose-dependent acute vascular pulmonary leakage and pleural effusion in rat models. Based on these studies, we speculate that the selective S1PR1 antagonism at least does not have hepatoprotective effect in hepatic IRI even if the type of animal models is different. Further studies are required to clarify these functions.

In conclusion, S1PR1 agonist treatment induces attenuation of hepatic IRI, which might be provided by preventing SEC damage, although the other pathways such as regulation of inflammatory/immune cells migration might be involved. As the role for the prevention of sinusoidal endothelial injury after hepatic IRI, S1PR1 agonism may be a therapeutic target.

Acknowledgment

Authors' contributions: T.I. and N.K. designed the study, performed the experiments and interpretation of data, and wrote the initial draft of the manuscript. H.K. and A.M. supported the first and corresponding authors to perform the experiments. All other authors contributed to data analysis and have critically reviewed the study design and the manuscript. All authors approved the final version of the manuscript and agreed to be accountable for all aspects of the work in ensuring that questions related to the accuracy or integrity of any part of the work are appropriately investigated and resolved.

Funding: This work was supported by JSPS KAKENHI Grant Number JP16K10569.

Supplementary data

Supplementary data related to this article can be found at https://doi.org/10.1016/j.jss.2017.09.048.

Disclosure

The authors report no proprietary or commercial interest in any product mentioned or concept discussed in this article.

REFERENCES

1. Selzner N, Rudiger H, Graf R, Clavien PA. Protective strategies against ischemic injury of the liver. *Gastroenterology*. 2003;125:917–936.
2. Montalvo-Jave EE, Escalante-Tattersfield T, Ortega-Salgado JA, Piña E, Geller DA. Factors in the pathophysiology of the liver ischemia-reperfusion injury. *J Surg Res*. 2008;147:153–159.
3. Smedsrød B. Clearance function of scavenger endothelial cells. *Comp Hepatol*. 2004;3(Suppl l):S22.
4. Singleton PA, Dudek SM, Chiang ET, Garcia JG. Regulation of sphingosine 1-phosphate-induced endothelial cytoskeletal rearrangement and barrier enhancement by S1P1 receptor, PI3 kinase, Tiam1/Rac1, and alpha-actinin. *FASEB J*. 2005;19:1646–1656.
5. Igarashi J, Michel T. Sphingosine-1-phosphate and modulation of vascular tone. *Cardiovasc Res*. 2009;82:212–220.
6. Potì F, Simoni M, Nofer JR. Atheroprotective role of high-density lipoprotein (HDL)-associated sphingosine-1-phosphate (S1P). *Cardiovasc Res*. 2014;103:395–404.
7. Matloubian M, Lo CG, Cinamon G, et al. Lymphocyte egress from thymus and peripheral lymphoid organs is dependent on S1P receptor 1. *Nature*. 2004;427:355–360.
8. Sanna MG, Liao J, Jo E, et al. Sphingosine 1-phosphate (S1P) receptor subtypes S1P1 and S1P3, respectively, regulate lymphocyte recirculation and heart rate. *J Biol Chem*. 2004;279:13839–13848.
9. Lien YH, Yong KC, Cho C, Igarashi S, Lai LW. S1P (1)-selective agonist, SEW2871, ameliorates ischemic acute renal failure. *Kidney Int*. 2006;69:1601–1608.
10. Lai LW, Yong KC, Igarashi S, Lien YH. A sphingosine-1-phosphate type 1 receptor agonist inhibits the early T-cell transient following renal ischemia-reperfusion injury. *Kidney Int*. 2007;71:1223–1231.
11. Hofmann U, Burkard N, Vogt C, et al. Protective effects of sphingosine-1-phosphate receptor agonist treatment after myocardial ischemia-reperfusion. *Cardiovasc Res*. 2009;83:285–293.
12. Ni Q, Yuan B, Liu T, et al. Sphingosine-1-phosphate receptor 1 agonist SEW2871 prolongs heterotopic heart allograft survival in mice. *Int Immunopharmacol*. 2015;26:37–42.
13. Samarska IV, Bouma HR, Buikema H, et al. S1P1 receptor modulation preserves vascular function in mesenteric and coronary arteries after CPB in the rat independent of depletion of lymphocytes. *PLoS One*. 2014;9:e97196.
14. Zou L, Ke L, Wu C, et al. SEW2871 alleviates the severity of caerulein-induced acute pancreatitis in mice. *Biol Pharm Bull*. 2015;38:1012–1019.
15. Liu S, Rockey DC. Cicletanine stimulates eNOS phosphorylation and NO production via Akt and MAP kinase/Erk signaling in sinusoidal endothelial cells. *Am J Physiol Gastrointest Liver Physiol*. 2013;305:G163–G171.
16. Nowatari T, Murata S, Nakayama K, et al. Sphingosine 1-phosphate has anti-apoptotic effect on liver sinusoidal endothelial cells and proliferative effect on hepatocytes in a paracrine manner in human. *Hepatol Res*. 2015;45:1136–1145.
17. Argraves KM, Gazzolo PJ, Groh EM, et al. High density lipoprotein-associated sphingosine 1-phosphate promotes endothelial barrier function. *J Biol Chem*. 2008;283:25074–25081.
18. Matsuda A, Kuriyama N, Kato H, et al. Comparative study on the cytoprotective effects of activated protein C treatment in nonsteatotic and steatotic livers under ischemia-reperfusion injury. *Biomed Res Int*. 2015;2015:635041.
19. Hamada T, Fondevila C, Busuttil RW, Coito AJ. Metalloproteinase-9 deficiency protects against hepatic ischemia/reperfusion injury. *Hepatology*. 2008;47:186–198.

20. Suzuki S, Nakamura S, Koizumi T, et al. The beneficial effect of a prostaglandin I2 analog on ischemic rat liver. *Transplantation*. 1991;52:979–983.
21. Chen SW, Park SW, Kim M, Brown KM, D'Agati VD, Lee HT. Human heat shock protein 27 overexpressing mice are protected against hepatic ischemia and reperfusion injury. *Transplantation*. 2009;87:1478–1487.
22. Duarte S, Hamada T, Kuriyama N, Busuttil RW, Coito AJ. TIMP-1 deficiency leads to lethal partial hepatic ischemia and reperfusion injury. *Hepatology*. 2012;56:1074–1085.
23. Kato H, Duarte S, Liu D, Busuttil RW, Coito AJ. Matrix Metalloproteinase-2 (MMP-2) gene deletion Enhances MMP-9 Activity, Impairs PARP-1 degradation, and exacerbates hepatic ischemia and reperfusion injury in mice. *PLoS One*. 2015;10:e0137642.
24. Braet F, Kalle WH, De Zanger RB, et al. Comparative atomic force and scanning electron microscopy: an investigation on fenestrated endothelial cells in vitro. *J Microsc*. 1996;181:10–17.
25. Park SW, Kim M, Chen SW, D'Agati VD, Lee HT. Sphinganine-1-phosphate attenuates both hepatic and renal injury induced by hepatic ischemia and reperfusion in mice. *Shock*. 2010;33:31–42.
26. Park SW, Kim M, Chen SW, Brown KM, D'Agati VD, Lee HT. Sphinganine-1-phosphate protects kidney and liver after hepatic ischemia and reperfusion in mice through S1P1 receptor activation. *Lab Invest*. 2010;90:1209–1224.
27. Martin M, Mory C, Prescher A, Wittekind C, Fiedler M, Uhlmann D. Protective effects of early CD4(+) T cell reduction in hepatic ischemia/reperfusion injury. *J Gastrointest Surg*. 2010;14:511–519.
28. Zheng DM, Kitamura T, Ikejima K, et al. Sphingosine 1-phosphate protects rat liver sinusoidal endothelial cells from ethanol-induced apoptosis: role of intracellular calcium and nitric oxide. *Hepatology*. 2006;44:1278–1287.
29. Xu M, Waters CL, Hu C, Wysolmerski RB, Vincent PA, Minnear FL. Sphingosine 1-phosphate rapidly increases endothelial barrier function independently of VE-cadherin but requires cell spreading and Rho kinase. *Am J Physiol Cell Physiol*. 2007;293: C1309–C1318.
30. Tobia C, Chiodelli P, Nicoli S, et al. Sphingosine-1-phosphate receptor-1 controls venous endothelial barrier integrity in zebrafish. *Arterioscler Thromb Vasc Biol*. 2012;32:e104–e116.
31. Lee MJ, Evans M, Hla T. The inducible G protein-coupled receptor edg-1 signals via the G (i)/mitogen-activated protein kinase pathway. *J Biol Chem*. 1996;19:11272–11279.
32. Morales-Ruiz M, Lee MJ, Zollner S, et al. Sphingosine 1-phosphate activates Akt, nitric oxide production, and chemotaxis through a Gi protein/phosphoinositide 3-kinase pathway in endothelial cells. *J Biol Chem*. 2001;276:19672–19677.
33. Jung B, Obinata H, Galvani S, et al. Flow-regulated endothelial S1P receptor-1 signaling sustains vascular development. *Dev Cell*. 2012;23:600–610.
34. Ham A, Kim M, Kim JY, et al. Selective deletion of the endothelial sphingosine-1-phosphate 1 receptor exacerbates kidney ischemia-reperfusion injury. *Kidney Int*. 2014;85:807–823.
35. Bigaud M, Dincer Z, Bollbuck B, et al. Pathophysiological consequences of a break in S1P1-Dependent homeostasis of vascular permeability revealed by S1P1 competitive antagonism. *PLoS One*. 2016;11:e0168252.